Clim. Past Discuss., 10, 2397–2416, 2014
www.clim-past-discuss.net/10/2397/2014/
doi:10.5194/cpd-10-2397-2014

Climate of the Past
Discussions
Open Access

Links between CO_2, glaciation and water flow: reconciling the Cenozoic history of the Antarctic Circumpolar Current

J.-B. Ladant, Y. Donnadieu, and C. Dumas

Laboratoire des Sciences du Climat et de l'Environnement, CEA-CNRS-UVSQ, CEA Saclay, Gif-sur-Yvette, France

Received: 25 April 2014 – Accepted: 12 May 2014 – Published: 22 May 2014

Correspondence to: J.-B. Ladant (jean-baptiste.ladant@lsce.ipsl.fr)

Published by Copernicus Publications on behalf of the European Geosciences Union.

Abstract

The timing of the onset of the Antarctic Circumpolar Current (ACC) is a crucial event of the Cenozoic because of its cooling and isolating effect over Antarctica. It is intimately related to the glaciations occurring throughout the Cenozoic from the Eocene–Oligocene (EO) transition (≈34 Ma) to the middle Miocene glaciations (≈13.9 Ma). However, the exact timing of the onset remains debated with evidence for a late Eocene set up contradicting others data pointing to an occurrence closer to the Oligocene–Miocene (OM) boundary. In this study, we show the potential impact of the Antarctic ice sheet on the initiation of a proto-ACC at the EO boundary. Our results reveal that the regional cooling effect of the ice sheet increases the sea ice formation, which disrupts the meridional density gradient in the Southern Ocean and leads to the onset of a circumpolar current and its progressive strengthening. We also suggest that subsequent variations in atmospheric CO_2, ice sheet volumes and tectonic reorganizations may have affected the ACC intensity after the Eocene–Oligocene transition, which in turn may provide an explanation for the second initiation of the ACC at the Oligocene–Miocene boundary and may reconcile evidence supporting both early Oligocene and early Miocene onset of the ACC.

1 Introduction

Largest of all currents, the ACC has been studied for decades because of its non-negligible role in major climatic changes of the Cenozoic, notably at the Eocene–Oligocene transition (Kennett, 1977). If the opening of the Tasman Passage between Australia and Antarctica is relatively well constrained with progressive deepening between 35 and 30 Ma (Stickley et al., 2004), there are still numerous uncertainties in the timing of the opening of Drake Passage (Barker and Burrell, 1977; Lawver and Gahagan, 2003; Scher and Martin, 2006; Livermore et al., 2007). Consequently, the time evolution of the ACC between the Eocene and the Miocene remains unclear. Some

CPD
10, 2397–2416, 2014

studies have proposed an onset at the earliest Oligocene (e.g. Florindo and Roberts, 2005) while others tend to point the initiation toward late Oligocene or early Miocene (Pfuhl and McCave, 2005; Lyle et al., 2007; Scher and Martin, 2008). On a modelling side, Toggweiler and Bjornsson (2000) found that the opening of Drake Passage had a cooling effect over southern high latitudes but DeConto and Pollard (2003b) showed that possible changes in ocean heat transport due to gateways opening only had a limited impact on the Eocene–Oligocene Antarctic glaciation. This opinion was subsequently corroborated by Huber and Nof (2006). More recently, Hill et al. (2013) have argued that paleogeographic constraints prevented ACC initiation until late Oligocene while Lefebvre et al. (2012) investigated the effect of a decrease in atmospheric CO_2 concentration on the onset of the ACC and found that this current was not triggered by CO_2 typical of late Eocene, hence delaying its initiation to late Oligocene under colder climatic conditions.

Here we study the impact of the Antarctic ice sheet (AIS) growth at the Eocene–Oligocene boundary on the potential initiation of the ACC. The AIS has the potential to provide regionally colder conditions which could substitute the decrease in atmospheric CO_2 (Lefebvre et al., 2012) as trigger of the ACC.

2 Models and experiments

In this study, we use the mixed-resolution GCM FOAM (Fast Ocean Atmosphere Model) to realize coupled runs investigating the ice sheet growth effect on the oceanic circulation around Antarctica at the Eocene–Oligocene boundary. The atmospheric component runs on a 4.5° by 7.5° grid with 18 vertical levels. It is a modified version of the parallelized NCAR's CCM2 model so that the atmospheric physics is equivalent to CCM3. The highly efficient ocean component is dynamically similar to the Modular Ocean Model of GFDL (Jacob, 1997). It runs on a 1.4° by 2.8° grid with 12 of the 24 vertical levels in the upper 1000 m. The sea ice model uses the thermodynamics of NCAR's CSIM 2.2.6. FOAM has been used to successfully simulate present-day climate (e.g., Zhang et al., 2005) as well as paleoclimates (Poulsen et al., 2003; Chaboureau et al., 2012; Dera and Donnadieu, 2012).

In this paper, we aim at deciphering the impact of a growing ice sheet on the Southern ocean circulation and particularly if it allows the development of the ACC. The initiation threshold for the Eocene–Oligocene Antarctic ice sheet has been shown to be close to 800 ppm (Gasson et al., 2014; DeConto and Pollard, 2003a). We therefore set up GCM runs with atmospheric CO_2 concentration of 560 ppm (2x Preindustrial Atmospheric Levels) and 840 ppm (3x PAL) but also 1140 ppm (4x PAL), which corresponds to pre-transition levels (Pagani et al., 2011). Different ice sheet sizes have been prescribed over Antarctica (Table 1), ranging from a small size in the 1120 ppm case to a full ice sheet in the 560 ppm case. The maximum ice sheet size at 1120 ppm is small compared to the large maximum ice sheet size prescribed at 840 ppm or the full ice sheet prescribed at 560 ppm. Indeed, small ephemeral glaciation may have existed during the Eocene (Tripati et al., 2005) but did not reach the Antarctic coastline (Miller et al., 2005). This justifies the ice sheet geometry we use here (Fig. 1). The corresponding approximate ice volume prescribed for each ice sheet simulation can be found in Table 1.

The model is initialized with the Early Oligocene paleogeography used by Lefebvre et al. (2012) with already opened southern gateways. Mean depth of both gateways is 1600 m. The only change lies in the topography of Antarctica, which is obtained by isostatically removing present-day ice sheet (Fig. 1). The solar constant is reduced to 1361 $W m^{-2}$ and the Earth orbit has the following parameters (DeConto et al., 2007): eccentricity = 0.05, obliquity = 24.5°, perihelion in January. Other boundary conditions are kept at modern values.

3 Results

A control simulation regarding the ACC features with FOAM has been detailed in a previous study (Lefebvre et al., 2012). This preindustrial run yields realistic results when compared to observations and IPCC-AR4 coupled simulations (see details in Lefebvre et al., 2012) transport in the control run is 113 Sv at Drake Passage and 136 Sv at Tasman Passage for the entire water column. Consistently with the work of Lefebvre et al. (2012), the intensity of the ice-free Antarctic water flow at Drake and Tasman passages reaches very low values for the high atmospheric CO_2 concentrations typical of the EO boundary. Interestingly, for both 2 and 3x PAL, the ice sheet effect on the flow intensity is clear whereas the presence of ice at 4x PAL only has a very weak effect. Indeed, at 1120 ppm of CO_2, the water transport remains close to 10 Sv both at Drake and Tasman passages, whatever amount of ice is present over the continent (Table 1). At 3x PAL, there is a gradual water transport increase as the ice sheet grows. This growth results in an increase in the zonal flow intensity with almost a doubling at each increase except for the last ice sheet size (Table 1). At 2x PAL, the increase is even stronger for the two prescribed ice sheets. From an initial 8 Sv (also at Drake Passage), the transport reaches 42 Sv with a large ice sheet and 54 Sv for the full ice sheet (Table 1). In all simulations, the trend in the evolution of the flow intensity calculated across Tasman Passage is similar to the one described at Drake Passage, likely reflecting the onset of a continuous circumpolar current.

Profound changes in ocean circulation occur between the initial experiments and the following runs (Fig. 2). We will focus on the 560 ppm simulation, the average CO_2 threshold required to grow a full Antarctic ice sheet (Gasson et al., 2014). In the initial ice-free run, the ocean circulation around Antarctica displays no ACC or proto-ACC whatsoever. Some eastward transport of water of low intensity occurs at the Drake and Tasman gateways (Table 1). After crossing Tasman Passage, surface waters are deflected northward to join the south Pacific gyre, as previously noted by Hill et al. (2013). Only a small part of this proto-Humbolt current effectively crosses Drake Passage. The progressive build-up of the Antarctic ice sheet sets in place a proto-Ross gyre which drags waters away from the Tasman Passage and prevents them from being deflected northward. Consequently, an eastward current in the Southern Pacific Ocean is created which brings much more water through Drake Passage as well. After Drake

CPD
10, 2397–2416, 2014

Passage, waters join the eastward flowing current south of Africa until it reaches Australia, which completes the circulation. A proto-Weddell gyre forms in the Atlantic sector of the Southern Ocean once a fully-grown ice sheet is established. The eastern and north-eastern parts of the gyre strengthen the flow across Drake Passage as well the wind-driven eastward current flowing in the Atlantic and Indian sectors. The proto-Ross gyre is also reinforced.

The vertical structure of water transport provides support to the current reorganization into a past analogue of the modern ACC following the ice sheet build-up. Zonal fluxes of water at cross-sectional areas located at Drake and Tasman gateways (Fig. 3) reveals that the progressive ice sheet growth and subsequent feedbacks enable a similar although weaker than modern circulation of waters around Antarctica. When no ice is present on the continent, there are only very weak eastward fluxes across the gateways. When an ice sheet of large size has grown, water transport through Drake and Tasman passages increases dramatically and the water starts to be significantly advected eastward on the whole water column. With the full ice sheet, transport intensity increases all around Antarctica to reach up to half modern day intensity at Drake and Tasman passages.

The main driving mechanism of the ACC has been subject to intense debate these past decades. Among the firsts, Munk and Palmén (1951) have proposed that bottom topography could balance the eastward wind stress while Stommel (1957) invoked wind stress curl through Sverdrup transport. Studies have shown the large impact of winds (e.g. Gnanadesikan and Hallberg, 2000) and others pointed out buoyancy forcing (e.g. Gent et al., 2001). Therefore, it is likely that the ACC is driven by a complex balance between wind forcing, thermohaline-driven circulation and bottom topography (Cai and Baines, 1996).

The initiation of the Antarctic ice sheet has been shown to greatly enhance regional sea ice formation (DeConto et al., 2007). Here, we attribute the development of this proto-ACC to the increase in sea ice caused by the Antarctic glaciation. On Fig. 4 is represented the winter sea ice extension for the 560 ppm ice-free and full ice sheet

CPD
10, 2397–2416, 2014

Reconciling the Cenozoic history of the ACC

J.-B. Ladant et al.

simulations. Sea ice increases all around the continent (mean winter sea ice cover is extended by more than 75 %, see Fig. 4), notably in the modern location of the Ross and Ronne-Filchner ice shelves and in the Atlantic and Indian sector of the Southern Ocean. As demonstrated by Lefebvre et al. (2012) to explain the increasing ACC transport under decreasing atmospheric pCO_2, sea ice formation, through brine rejection process, creates cold and salty hence denser waters, which increases the meridional density gradient and consequently the ACC (Fig. 5).

4 Discussion

Our results highlight the effects of the Antarctic glaciation on a proto-ACC through extended sea ice formation. Transport through Drake and Tasman passages in our 2x full ice sheet control simulation is similar to the 2x Rupelian (i.e., late Eocene/early Oligocene paleogeography with a glaciated Antarctica) control simulation of Hill et al. (2013). Interestingly, they do not attribute this transport to the development of a proto-ACC. This is easily conceivable as the flow through Drake and Tasman passages in their simulations is already similar prior to the glaciation (see Hill et al., 2013, Rupelian control vs. Rupelian noAIS simulation). Indeed, contrary to DeConto et al. (2007) and the present study, they do not find significant sea ice increase induced by the glaciation, which we think is likely to be the main driver of the onset and further strengthening of a proto-ACC. Many studies have now shown that the existence of the ACC was not required to trigger Antarctic glaciation and that the prominent driver was likely to be the abrupt decrease in atmospheric CO_2 (Huber et al., 2004; DeConto and Pollard, 2003b; Sijp et al., 2011). In our simulation, the glaciation triggers the development of quite a strong circumpolar current, which supports the initiation of a proto-ACC as soon as the late Eocene/early Oligocene as a feedback to the build-up of the Antarctic ice sheet induced by CO_2 fall.

Our results are in agreement with numerous existing records. Scher and Martin (2006) have proposed that the increase in ε_{Nd} values at ODP sites 1090 and 689

CPD
10, 2397–2416, 2014

(in the Atlantic sector of the Southern Ocean) around 41 Ma reflects an influx of Pacific shallow waters into the Atlantic (also noted by Diester-Haass and Zahn, 1996) requiring a shallow to intermediate Drake Passage (Eagles et al., 2006; Lagabrielle et al., 2009). Though the flux through Drake Passage is low (around 10 Sv), our ice-free simulations are consistent with a Pacific toward Atlantic water path as soon as Drake Passage opened, regardless of the CO_2 concentration.

Major Southern Hemisphere tectonic reorganizations occur close to the Eocene–Oligocene boundary with the opening and progressive deepening of the Tasman gateway (Stickley et al., 2004; Lawver and Gahagan, 2003) and the deepening of Drake Passage (Lawver and Gahagan, 2003; Livermore et al., 2007). In addition, Antarctic glaciation cooled the continent and the surrounding ocean leading to an increase in sea ice formation (DeConto et al., 2007; Houben et al., 2013). Our results support the development of a proto-ACC of moderate intensity following the build-up of the ice sheet, roughly coeval with the EO transition onset of the ACC suggested by, e.g., Latimer and Filippelli (2002), Diekmann et al. (2004) and more recently Borelli et al. (2014).

Some studies propose a later onset of the ACC. For example, Pfuhl and McCave (2005) analysed sediment grain size from South Tasman Rise (ODP Leg 189) and, based on the size increase around 23.9 Ma, concluded to an intensification of deep water currents related to the deepening of Drake Passage and the initiation of the ACC. Lyle et al. (2007) used sediments from an Upper Oligocene to Holocene piston core to place the onset of the ACC between 25 and 23 Ma. These findings are not necessarily at odds with the results of this study, which places the initiation of a proto-ACC earlier. Indeed, this proto-ACC does only reach up to half modern day intensity and therefore, estimates of the onset of the ACC at the Oligocene–Miocene (OM) boundary might in fact represent another increase in the proto-ACC intensity (as well as possible modifications of the pathway) under tectonic reorganizations such as further deepening of the Drake Passage and progressive widening of the Tasman gateway.

Moreover, Lefebvre et al. (2012) reported a strong sensitivity of the ACC to atmospheric carbon dioxide concentration. To test the possibility that subsequent variations in Oligocene–Miocene pCO_2 (Zhang et al., 2013) have affected the intensity of the proto-ACC, we carried out another simulation with the same full ice sheet as in the 560 ppm simulation but with a CO_2 concentration of 1120 ppm. Interestingly, compared to the full ice sheet 560 ppm experiment, the proto-ACC transport decreases markedly by roughly a factor of three at both Drake (from 54 to 17 Sv) and Tasman (from 59 to 22 Sv) passages because the rise in atmospheric CO_2 counterbalances the impact of the ice sheet, by providing warmer conditions that limit the extension of sea ice formation.

We can then infer that the coupled effect of ice sheet and CO_2 could have favoured times of a somewhat strong proto-ACC (e.g. at the EO transition) but the successive variations in atmospheric pCO_2 and possible subsequent melting of some parts of the Antarctic ice sheet might have provoked a return to a much weaker circumpolar current. Additionally, the complex tectonic evolution of Drake Passage has surely played a role in possible variations of the proto-ACC intensity. Lagabrielle et al. (2009) notably showed that the temporary constriction of Drake Passage between approximately 29 and 22 Ma could have led to a decrease in the proto-ACC intensity, which would be in agreement with a second onset close to the Oligocene–Miocene boundary (Pfuhl and McCave, 2005; Lyle et al., 2007). However, to our knowledge, no study has yet analysed material spanning both the EO and the OM transitions in search for ACC initiation. Future studies should hence work on resolving this issue to provide a continuous record of potential ACC imprints.

5 Conclusions

Since Kennett's hypothesis of an ACC control on the major Antarctic glaciation at the EO transition, the timing of its initiation has been matter of debate. Due to the complex tectonic evolution of the Drake and Tasman passages, reconstructing the full history of the Southern Ocean is still quite complicated. In this study, we show that the progressive growth of the ice sheet at the EO boundary leads to the initiation of a proto-ACC

CPD
10, 2397–2416, 2014

of up to half modern day transport. The main mechanism invoked to explain this rise involves increased sea ice formation around Antarctica consecutive to the glaciation (DeConto et al., 2007), which modifies the meridional density gradient and leads to a stronger circumpolar current (Lefebvre et al., 2012). These findings are in favour of an ACC onset close to the EO boundary (or at least a non-negligible circumpolar current reorganization) but do not preclude studies invoking a later onset of the ACC. Indeed, we have shown that a rise in atmospheric CO_2 after the EO transition (Pearson et al., 2009) reduces the intensity of this proto-ACC. Additionally, possible waxing and waning of the ice sheet during the Oligocene seen in $\delta^{18}O$ (Wade and Pälike, 2004) and sea level records (Miller et al., 2005) as well as paleogeographic changes (Hill et al., 2013) and Glacial Isostatic Adjustment-induced ocean changes due to the ice sheet build-up (Rugenstein et al., 2014) are also likely to have had a great influence on the intensity of this circumpolar flow. Possible shutdown or slowdown of the ACC between approximately 29 and 22 Ma has also been suggested due to temporary constriction of Drake Passage (Lagabrielle et al., 2009) and can be invoked to reconcile this apparent discrepancy in the timing of the ACC: the first onset of the circumpolar current would then have occurred close to the EOT (Latimer and Filippelli, 2002; Katz et al., 2011; Borrelli et al., 2014) following Antarctic glaciation before a period of possible variations in its intensity under changes in pCO_2 and ice sheet size ending by a period of progressive slowdown (Lagabrielle et al., 2009). The Oligocene–Miocene boundary would then mark the second onset of the ACC (Pfuhl and McCave, 2005; Lyle et al., 2007) predating the evolution towards its modern features (Heinrich et al., 2011; Dalziel et al., 2013).

Acknowledgements. We thank the CEA/CCRT for providing access to the HPC resources of TGCC under the allocation 2014-012212 made by GENCI. This research was funded by a CEA PhD grant CFR.

CPD
10, 2397–2416, 2014

References

Barker, P. and Burrell, J.: The opening of Drake passage, Mar. Geol., 25, 15–34, 1977.

Borrelli, C., Cramer, B. S., and Katz, M. E.: Bipolar Atlantic deepwater circulation in the middle–late Eocene: effects of Southern Ocean gateway openings, Paleoceanography, 29, 308–327, doi:10.1002/2012pa002444, 2014.

Cai, W. and Baines, P. G.: Interactions between thermohaline- and wind-driven circulations and their relevance to the dynamics of the Antarctic circumpolar current, in a coarse-resolution global ocean general circulation model, J. Geophys. Res., 101, 14073, doi:10.1029/96jc00669, 1996.

Chaboureau, A.-C., Donnadieu, Y., Sepulchre, P., Robin, C., Guillocheau, F., and Rohais, S.: The Aptian evaporites of the South Atlantic: a climatic paradox?, Clim. Past, 8, 1047–1058, doi:10.5194/cp-8-1047-2012, 2012.

Dalziel, I. W. D., Lawver, L. A., Pearce, J. A., Barker, P. F., Hastie, A. R., Barfod, D. N., Schenke, H. W., and Davis, M. B.: A potential barrier to deep Antarctic circumpolar flow until the late Miocene?, Geology, 41, 947–950, doi:10.1130/g34352.1, 2013.

DeConto, R. M. and Pollard, D.: A coupled climate–ice sheet modeling approach to the Early Cenozoic history of the Antarctic ice sheet, Palaeogeogr. Palaeocl., 198, 39–52, doi:10.1016/s0031-0182(03)00393-6, 2003a.

DeConto, R. M. and Pollard, D.: Rapid Cenozoic glaciation of Antarctica induced by declining atmospheric CO_2, Nature, 421, 245–249, 2003b.

DeConto, R., Pollard, D., and Harwood, D.: Sea ice feedback and Cenozoic evolution of Antarctic climate and ice sheets, Paleoceanography, 22, PA3214, doi:10.1029/2006pa001350, 2007.

Dera, G. and Donnadieu, Y.: Modeling evidences for global warming, Arctic seawater freshening, and sluggish oceanic circulation during the Early Toarcian anoxic event, Paleoceanography, 27, PA2211, doi:10.1029/2012pa002283, 2012.

Diekmann, B., Kuhn, G., Gersonde, R., and Mackensen, A.: Middle Eocene to early Miocene environmental changes in the sub-Antarctic Southern Ocean: evidence from biogenic and terrigenous depositional patterns at ODP Site 1090, Global Planet. Change, 40, 295–313, 2004.

Diester-Haass, L. and Zahn, R.: Eocene–Oligocene transition in the Southern Ocean: history of water mass circulation and biological productivity, Geology, 24, 163–166, 1996.

CPD
10, 2397–2416, 2014

Eagles, G., Livermore, R., and Morris, P.: Small basins in the Scotia Sea: the Eocene Drake passage gateway, Earth Planet. Sc. Lett., 242, 343–353, 2006.
Florindo, F. and Roberts, A. P.: Eocene–Oligocene magnetobiochronology of ODP Sites 689 and 690, Maud Rise, Weddell Sea, Antarctica, Geol. Soc. Am. Bull., 117, 46–66, doi:10.1130/b25541.1, 2005.
Gasson, E., Lunt, D. J., DeConto, R., Goldner, A., Heinemann, M., Huber, M., LeGrande, A. N., Pollard, D., Sagoo, N., Siddall, M., Winguth, A., and Valdes, P. J.: Uncertainties in the modelled CO_2 threshold for Antarctic glaciation, Clim. Past, 10, 451–466, doi:10.5194/cp-10-451-2014, 2014.
Gent, P. R., Large, W. G., and Bryan, F. O.: What sets the mean transport through Drake passage?, J. Geophys. Res., 106, 2693–2712, doi:10.1029/2000jc900036, 2001.
Gnanadesikan, A. and Hallberg, R. W.: On the relationship of the circumpolar current to Southern Hemisphere winds in coarse-resolution ocean models, J. Phys. Oceanogr., 30, 2013–2034, 2000.
Heinrich, S., Zonneveld, K. A. F., Bickert, T., and Willems, H.: The Benguela upwelling related to the Miocene cooling events and the development of the Antarctic circumpolar current: evidence from calcareous dinoflagellate cysts, Paleoceanography, 26, PA3209, doi:10.1029/2010pa002065, 2011.
Hill, D. J., Haywood, A. M., Valdes, P. J., Francis, J. E., Lunt, D. J., Wade, B. S., and Bowman, V. C.: Paleogeographic controls on the onset of the Antarctic circumpolar current, Geophys. Res. Lett., 40, 1–6, doi:10.1002/grl.50941, 2013.
Houben, A. J. P., Bijl, P. K., Pross, J., Bohaty, S. M., Passchier, S., Stickley, C. E., Rohl, U., Sugisaki, S., Tauxe, L., van de Flierdt, T., Olney, M., Sangiorgi, F., Sluijs, A., Escutia, C., and Brinkhuis, H.: Reorganization of Southern Ocean plankton ecosystem at the onset of Antarctic glaciation, Science, 340, 341–344, doi:10.1126/science.1223646, 2013.
Huber, M. and Nof, D.: The ocean circulation in the Southern Hemisphere and its climatic impacts in the Eocene, Palaeogeogr. Palaeocl., 231, 9–28, 2006.
Huber, M., Brinkhuis, H., Stickley, C. E., Döös, K., Sluijs, A., Warnaar, J., Schellenberg, S. A., and Williams, G. L.: Eocene circulation of the Southern Ocean: was Antarctica kept warm by subtropical waters?, Paleoceanography, 19, PA4026, doi:10.1029/2004PA001014, 2004.
Jacob, R.: Low Frequency Variability in a Simulated Atmosphere Ocean System, PhD thesis, University of Wisconsin-Madison, Madison, Wisconsin, USA, 1997.

Katz, M. E., Cramer, B. S., Toggweiler, J. R., Esmay, G., Liu, C., Miller, K. G., Rosenthal, Y., Wade, B. S., and Wright, J. D.: Impact of Antarctic circumpolar current development on late paleogene ocean structure, Science, 332, 1076–1079, doi:10.1126/science.1202122, 2011.

Kennett, J. P.: Cenozoic evolution of Antarctic glaciation, the circum-Antarctic Ocean, and their impact on global paleoceanography, J. Geophys. Res., 82, 3843–3860, doi:10.1029/JC082i027p03843, 1977.

Lagabrielle, Y., Goddéris, Y., Donnadieu, Y., Malavieille, J., and Suarez, M.: The tectonic history of Drake passage and its possible impacts on global climate, Earth Planet. Sc. Lett., 279, 197–211, doi:10.1016/j.epsl.2008.12.037, 2009.

Latimer, J. C., and Filippelli, G. M.: Eocene to Miocene terrigenous inputs and export production: Geochemical evidence from ODP Leg 177, Site 1090, Palaeogeogr. Palaeocl., 182, 151–164, 2002.

Lawver, L. A. and Gahagan, L. M.: Evolution of Cenozoic seaways in the circum-Antarctic region, Palaeogeogr. Palaeocl., 198, 11–37, doi:10.1016/s0031-0182(03)00392-4, 2003.

Lefebvre, V., Donnadieu, Y., Sepulchre, P., Swingedouw, D., and Zhang, Z.-S.: Deciphering the role of southern gateways and carbon dioxide on the onset of the Antarctic circumpolar current, Paleoceanography, 27, PA4201, doi:10.1029/2012pa002345, 2012.

Livermore, R., Hillenbrand, C.-D., Meredith, M., and Eagles, G.: Drake passage and cenozoic climate: an open and shut case?, Geochem. Geophys. Geosy., 8, Q01005, doi:10.1029/2005GC001224, 2007.

Lyle, M., Gibbs, S., Moore, T. C., and Rea, D. K.: Late Oligocene initiation of the Antarctic circumpolar current: evidence from the South Pacific, Geology, 35, 691–694, 2007.

Miller, K. G., Kominz, M. A., Browning, J. V., Wright, J. D., Mountain, G. S., Katz, M. E., Sugarman, P. J., Cramer, B. S., Christie-Blick, N., and Pekar, S. F.: The Phanerozoic record of global sea-level change, Science, 310, 1293–1298, 2005.

Munk, W. H. and Palmén, E.: Note on the dynamics of the Antarctic circumpolar current, Tellus, 3, 53–55, 1951.

Pagani, M., Huber, M., Liu, Z., Bohaty, S. M., Henderiks, J., Sijp, W., Krishnan, S., and DeConto, R. M.: The role of carbon dioxide during the onset of Antarctic glaciation, Science, 334, 1261–1264, doi:10.1126/science.1203909, 2011.

Pearson, P. N., Foster, G. L., and Wade, B. S.: Atmospheric carbon dioxide through the Eocene–Oligocene climate transition, Nature, 461, 1110–1113, doi:10.1038/nature08447, 2009.

CPD
10, 2397–2416, 2014

Reconciling the Cenozoic history of the ACC

J.-B. Ladant et al.

Pfuhl, H. A. and McCave, I. N.: Evidence for late Oligocene establishment of the Antarctic circumpolar current, Earth Planet. Sc. Lett., 235, 715–728, 2005.
Poulsen, C. J., Gendaszek, A. S., and Jacob, R. L.: Did the rifting of the Atlantic Ocean cause the cretaceous thermal maximum?, Geology, 31, 115–118, 2003.
Rugenstein, M., Stocchi, P., von der Heydt, A., Dijkstra H., Brinkhuis H., Emplacement of Antarctic ice sheet mass affects circumpolar ocean flow, Global Planet. Change, 118, 16–24, doi:10.1016/j.gloplacha.2014.03.011, 2014.
Scher, H. D. and Martin, E. E.: Timing and climatic consequences of the opening of Drake passage, Science, 312, 428–430, 2006.
Scher, H. D. and Martin, E. E.: Oligocene deep water export from the North Atlantic and the development of the Antarctic circumpolar current examined with neodymium isotopes, Paleoceanography, 23, PA1205, doi:10.1029/2006PA001400, 2008.
Sijp, W. P., England, M. H., and Huber, M.: Effect of the deepening of the Tasman gateway on the global ocean, Paleoceanography, 26, PA4207, doi:10.1029/2011PA002143, 2011.
Stickley, C. E., Brinkhuis, H., Schellenberg, S. A., Sluijs, A., Röhl, U., Fuller, M., Grauert, M., Huber, M., Warnaar, J., and Williams, G. L.: Timing and nature of the deepening of the Tasmanian gateway, Paleoceanography, 19, PA4027, doi:10.1029/2004pa001022, 2004.
Stommel, H.: A survey of ocean current theory, Deep-Sea Res., 4, 149–184, 1957.
Toggweiler, J. and Bjornsson, H.: Drake passage and palaeoclimate, J. Quaternary Sci., 15, 319–328, 2000.
Tripati, A., Backman, J., Elderfield, H., and Ferretti, P.: Eocene bipolar glaciation associated with global carbon cycle changes, Nature, 436, 341–346, doi:10.1038/nature03874, 2005.
Wade, B. S. and Pälike, H.: Oligocene climate dynamics, Paleoceanography, 19, PA4019, doi:10.1029/2004PA001042, 2004.
Zhang, Q., Yang, H., Zhong, Y., and Wang, D.: An idealized study of the impact of extratropical climate change on El Niño–Southern Oscillation, Clim. Dynam., 25, 869–880, doi:10.1007/s00382-005-0062-z, 2005.
Zhang, Y. G., Pagani, M., Liu, Z., Bohaty, S. M., and DeConto, R. M.: A 40-million-year history of atmospheric CO_2, Philos. T. Roy. Soc. A, 371, doi:10.1098/rsta.2013.0096, 2013.

Table 1. Water transport through Drake and Tasman gateways for each simulation.

CO_2 (ppm)	Ice sheet size (Approximate ice volume in 10^6 km^3)	Flow intensity at Drake Passage (Sv)	Flow intensity at Tasman Passage (Sv)
1120	Ice free	6	10
	Very small (3.5)	9	14
	Small (6)	10	15
840	Ice free	8	11
	Small (6)	14	18
	Medium (11)	29	38
	Large (16)	35	46
560	Ice free	8	13
	Large (15)	42	49
	Full (25)	54	59

CPD
10, 2397–2416, 2014

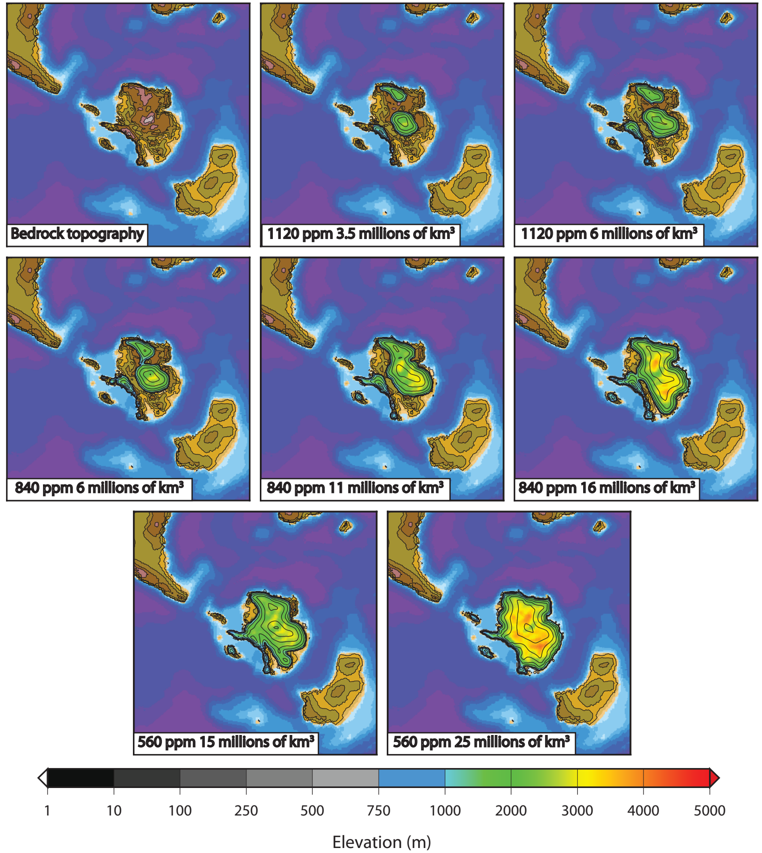

Figure 1. Bedrock topography of Antarctica and the different ice sheet prescribed at 1120, 840 and 560 ppm. Note that the different ice sheets are derived from preliminary runs at each CO_2, which results in different ice sheet shape and height for each CO_2. The 6 millions km^3 ice sheet at 1120 ppm is hence different from the 6 millions km^3 ice sheet at 840 ppm. The ice sheet volume is given to ease comparisons with Table 1 of the manuscript.

CPD
10, 2397–2416, 2014

Reconciling the Cenozoic history of the ACC

J.-B. Ladant et al.

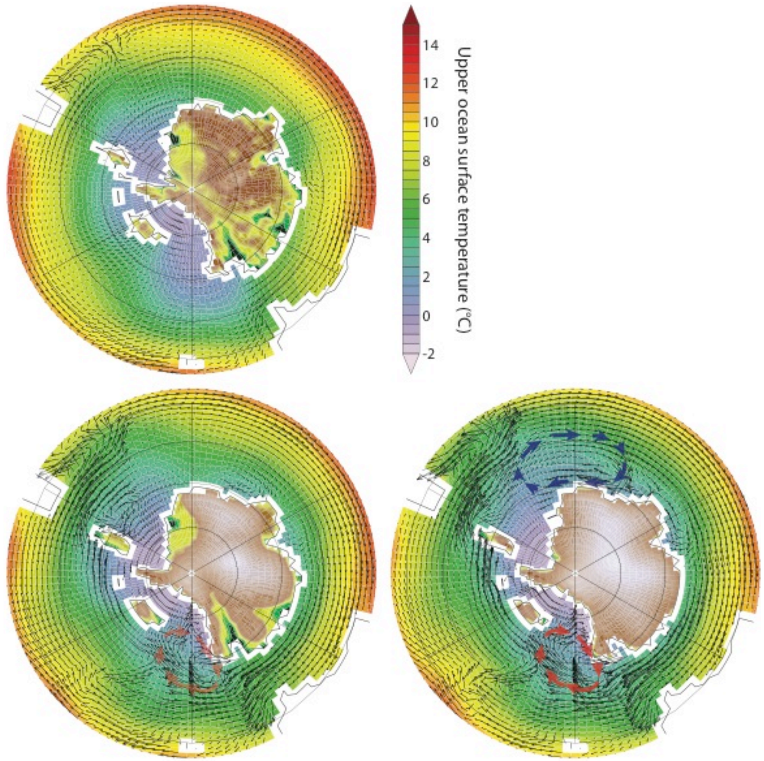

Figure 2. Surface (upper 75 m) ocean currents reorganization and temperature associated with the growth of the Antarctic ice sheet at 560 ppm. Ice free Antarctica (upper left), with a large ice sheet (lower left) or a full ice sheet (lower right). Proto-Ross and Weddell gyres are indicated in red and blue respectively. Note the strengthening of the proto-Ross gyre in the full ice sheet case, indicated by redder arrows.

CPD
10, 2397–2416, 2014

Reconciling the Cenozoic history of the ACC

J.-B. Ladant et al.

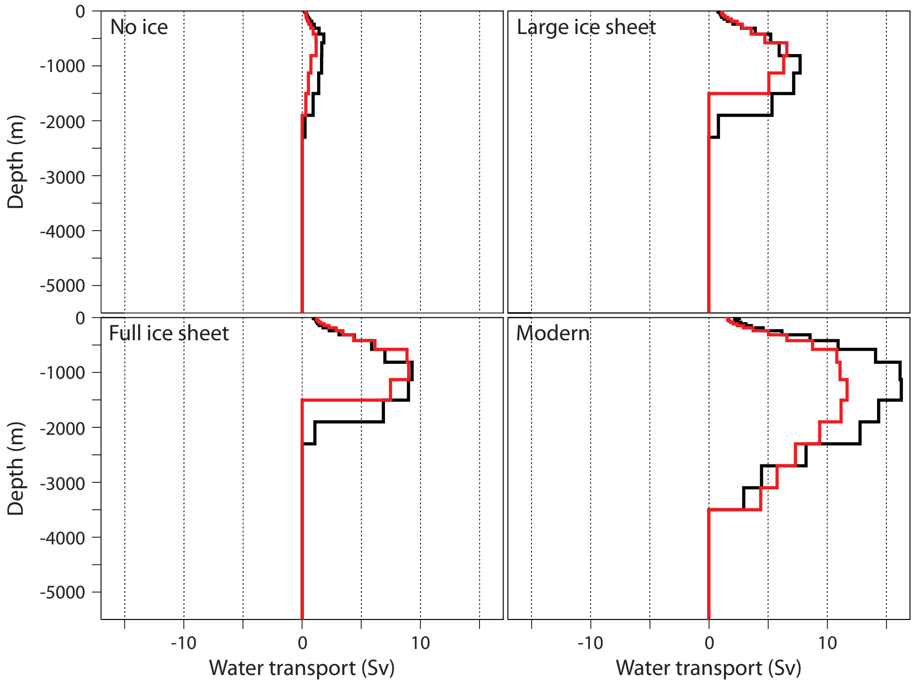

Figure 3. Zonal water transport through cross sectional areas located at Drake (red) and Tasman passages (black) for the 560 ppm simulations for **(a)** Ice free Antarctica; **(b)** with a large ice sheet; **(c)** with a full ice sheet; and **(d)** for the modern Antarctica of the control simulation (Lefebvre et al., 2012).

CPD
10, 2397–2416, 2014

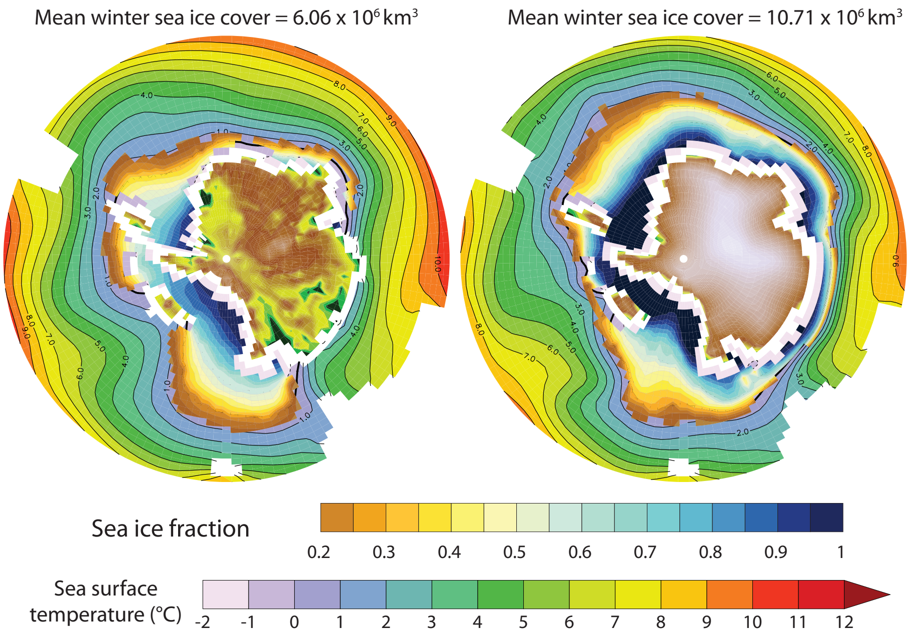

Figure 4. Sea ice extent and mean winter sea ice cover for the 560 ppm ice free (left) and full ice sheet (right) simulations.

CPD
10, 2397–2416, 2014

Reconciling the Cenozoic history of the ACC

J.-B. Ladant et al.

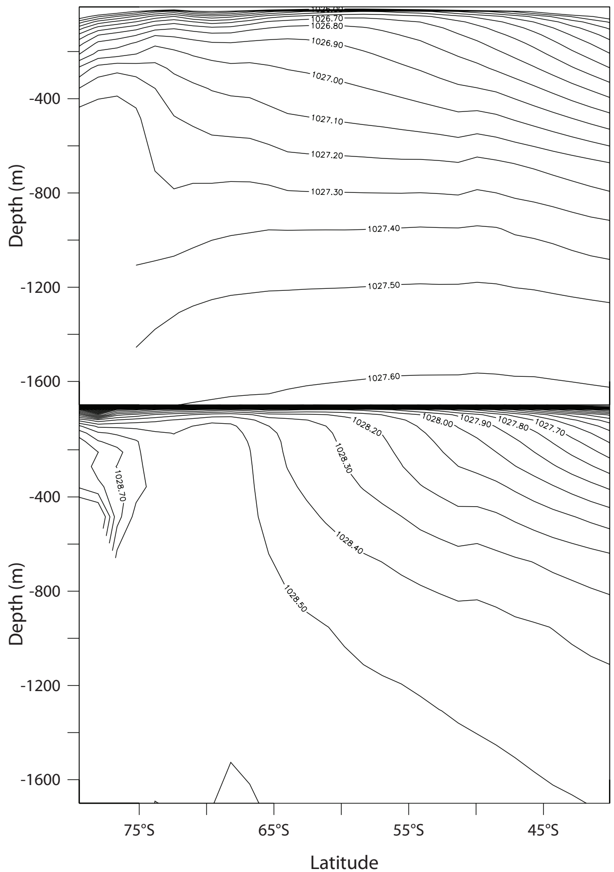

Figure 5. Zonally averaged seawater density profile for the 560 ppm ice free (upper panel) and full ice sheet (lower panel) simulations.

CPD
10, 2397–2416, 2014

Reconciling the Cenozoic history of the ACC

J.-B. Ladant et al.